1984–1997 *Nucleic Acids Research, 2013, Vol. 41, No. 3* *Published online 24 December 2012*
doi:10.1093/nar/gks1309

STA1, an *Arabidopsis* pre-mRNA processing factor 6 homolog, is a new player involved in miRNA biogenesis

Samir Ben Chaabane[1], Renyi Liu[2], Viswanathan Chinnusamy[2,3], Yerim Kwon[4], Joo-hyuk Park[4], Seo Yeon Kim[5], Jian-Kang Zhu[2,6,7], Seong Wook Yang[1,*] and Byeong-ha Lee[4,*]

[1]Department of Plant Biology and Biotechnology, Faculty of Life Science, University of Copenhagen, Thovanlsensvej 40, 1871 Frederiksberg, Copenhagen, Denmark, [2]Department of Botany and Plant Sciences, University of California, Riverside, CA 92521, USA, [3]Division of Plant Physiology, Indian Agricultural Research Institute, New Delhi 110012, India, [4]Department of Life Science, Sogang University, Seoul 121-742, Korea, [5]Department of Life Science, Ewha Womans University, Seoul 120-750, Korea, [6]Department of Horticulture and Landscape Architecture, University of Purdue, West Lafayette, IN 47907, USA and [7]Shanghai Center for Plant Stress Biology and Shanghai Institute of Plant Physiology and Ecology, Shanghai Institutes of Biological Sciences, Chinese Academy of Sciences, Shanghai, People's Republic of China

Received September 1, 2012; Revised November 15, 2012; Accepted November 16, 2012

ABSTRACT

MicroRNAs (miRNAs) are small regulatory RNAs that have important regulatory roles in numerous developmental and metabolic processes in most eukaryotes. In *Arabidopsis*, *DICER-LIKE1 (DCL1), HYPONASTIC LEAVES 1, SERRATE, HUA ENHANCER1* and *HASTY* are involved in processing of primary miRNAs (pri-miRNAs) to yield precursor miRNAs (pre-miRNAs) and eventually miRNAs. In addition to these components, mRNA cap-binding proteins, *CBP80/ABA HYPERSENSITIVE1* and *CBP20*, also participate in miRNA biogenesis. Here, we show that *STABILIZED1* (*STA1*), an *Arabidopsis* pre-mRNA processing factor 6 homolog, is also involved in the biogenesis of miRNAs. Similar to other miRNA biogenesis-defective mutants, *sta1-1* accumulated significantly lower levels of mature miRNAs and concurrently higher levels of pri-miRNAs than wild type. The dramatic reductions of mature miRNAs were associated with the accumulation of their target gene transcripts and developmental defects. Furthermore, *sta1-1* impaired splicing of intron containing pri-miRNAs and decreased transcript levels of *DCL1*. These results suggest that *STA1* is involved in miRNA biogenesis directly by functioning in pri-miRNA splicing and indirectly by modulating the *DCL1* transcript level.

INTRODUCTION

In plants, many growth and developmental processes are regulated by microRNA (miRNAs). These include development of rosette leaves, root development, apical dominancy of stem, auxin signaling, abscisic acid (ABA) responses, morphogenesis of flowers and arrangement of siliques (1–4). The responses of plants to abiotic stresses such as drought, high salinity, phosphate starvation and UV-B are also mediated by some miRNAs (5–10).

MiRNAs are generated from long primary transcripts [primary miRNAs (pri-miRNAs)] via precursor miRNAs (pre-miRNAs) through two-step processes involving at least five proteins [DICER-LIKE1 (DCL1), HYPONASTIC LEAVES 1 (HYL1), SERRATE (SE), HUA ENHANCER (HEN1) and HASTY (HST)] (11–16). DCL1 is the RNAse type III slicer that cleaves pri-miRNAs to produce pre-miRNAs and eventually miRNAs (17,18). HYL1 is a double-stranded RNA-binding protein with two RNA-binding domains for co-operative binding most likely to the miRNA/miRNA* duplex region. HYL1 interacts with SE and DCL1 through RNA-binding domain 2 (RBD2) for precise pri-miRNA processing (18–20). SE is a zinc-finger protein that enhances the accuracy of DCL1-dependent

*To whom correspondence should be addressed. Tel: +82 2 705 8794; Fax: +82 2 704 3601; Email: byeongha@sogang.ac.kr
Correspondence may also be addressed to Seong Wook Yang. Tel: +45 35 33 33 37; Fax: +45 35 33 33 00; Email: swyang@life.ku.dk

The authors wish it to be known that, in their opinion, the first two authors should be regarded as joint First Authors.

pri-miRNA processing together with HYL1 (18,21,22). HEN1 is a specific methyltransferase that adds a methyl group to the 2′-OH position of miRNA/miRNA* and siRNA/siRNA* duplexes. The HEN1-dependent methylation protects small RNA duplexes from unspecific addition of polyuridines and subsequent degradation (23). Finally, HST, the *Arabidopsis* homolog of the human nucleocytoplasmic transport factor Exportin-5 exports the miRNA/miRNA* duplex to cytoplasm (14).

Recently, two RNA-binding proteins were defined as components in miRNA biogenesis (24,25). One is DAWDLE (DDL), a type of fork-head associate domain (FHA) protein that interacts with DCL1 and functions in miRNA biogenesis, probably through stabilizing pri-miRNA transcript (24). Another is TOUGH (TGH) with G-patch and SWAP domains that promotes pri-miRNA recruitment to HYL1 and enhances the pri-miRNA processing efficiency as a component of the DCL1–HYL1–SE microprocessor complex (25).

The levels of pre-messenger RNAs (pre-mRNAs) in eukaryotes are tightly controlled by maturation (modification of nascent transcript with 5′-capping, splicing and 3′-polyadenylation) and stability. Likewise, pri-miRNAs are transcribed by RNA polymerase II and further modified by the addition of a 5′-seven methyl guanine cap and a polyadenosine tail at the 3′-end, and then processed by splicing in case of intron-containing nascent transcripts (26,27). Despite similarities in the maturation processes of pre-mRNAs and pri-miRNAs, their final destinations and functions are quite distinct. Mature mRNAs are exported to the cytoplasm and undergo a pioneer round of translation, and defective or improperly processed mRNAs are removed by the nonsense-mediated mRNA decaying pathway (28). In contrast, mature pri-miRNAs in plants are mostly retained in the nucleus for further processing into mature miRNAs and then exported to the cytoplasm (29,30). However, in plants very little is known about the maturation events from nascent transcripts to mature pri-miRNAs. Recently, a link between pre-mRNA processing and pri-miRNA processing emerged with the discovery of involvement of ABA HYPERSENSITIVE1 (ABH1)/CBP80 and CBP20 in pri-miRNA biogenesis (31). In addition to reduced pre-mRNA splicing efficiency, levels of pri-miRNAs are increased and mature miRNAs are reduced in *abh1*/*cbp80* and *cbp20* mutants as compared with wild-type (WT) plants (31). ABH1/CBP80 and CBP20 constitute a large complex, the nuclear cap-binding complex (CBC) that binds to the 5′-cap of pre-mRNAs (32). These results suggested that ABH1/CBP80 and CBP20 cap-binding proteins are involved in both pre-mRNA and pri-miRNA processing. Laubinger *et al.* (31) also suggested that *SE* has dual roles in pre-mRNA splicing and pri-miRNA processing and that *SE* might share a common mechanism with *CBC* or be a part of a larger cap-binding protein complex. Furthermore, inactivation of *ABH1*/*CBP80* and *CBP20* displayed significant reductions of ta-siRNAs along with their initiators, miR173 and miR390 (33). Despite the prominent reduction of ta-siRNAs that are important to sense post-transcriptional gene silencing, *ABH1*/*CBP80* is not involved in the sense-TGS pathway, suggesting that their roles may be limited to miRNA biogenesis (33).

The involvement of ABH1/CBP80 and CBP20 in pri-miRNA processing raises interesting questions as to whether other pre-mRNA processing proteins are also involved in pri-miRNA processing. To address these questions, we focused on *STABILIZED1* (*STA1*), a gene for pre-mRNA processing in *Arabidopsis*. *STA1* encodes a protein that is homologous to human U5 snRNP-associated 102-kDa protein (PRPF6), and the yeast pre-mRNA splicing factors, PRP1p (fission yeast) and Prp6p (budding yeast), and was shown to be important in pre-mRNA splicing and mRNA stability (34). In addition, the pleiotropic defects of development, chilling sensitivity and hypersensitivity to ABA were observed in *sta1-1*, a weak allele of *sta1* (34). Based on these initial clues, we investigated the possible role of *STA1* in splicing of pri-miRNAs and the biogenesis of miRNAs through a series of molecular and bioinformatic analyses in this study.

MATERIALS AND METHODS

Plant materials and growth conditions

se-1 (35), *hyl1-2* (SALK_ 064863) and *abh1-285* (SALK_ 024285) mutants of the Colombial-0 (Col-0) background and *sta1-1* with a single mutation in the Columbia-*gl1* background harboring the stress-responsive RD29A promoter-driven luciferase (Col-RD29A-LUC) were used in this study (34). Col-0 and Col-RD29A-LUC were considered the WT. Seeds were grown on Murashige and Skoog medium (1% sucrose and 0.8% agarose) after surface sterilization with sodium hypochlorite (7%). The seeds were stratified at 4°C for 3 days in dark and transferred to a growth chamber (16-h light and 8-h dark at 22°C). For cold treatment, plants were placed in an ice-filled insulated box for 24 h in a 4°C cold room.

RNA extraction and cDNA synthesis from total RNAs

Total RNA was extracted from the seedlings using RNeasy Plant Mini Kits (QIAGEN) or IQeasy Plant RNA extraction Mini Kit (iNtRON). Total RNAs from Col-0, *se-1*, *hyl1-2* and *sta1-1* were used as templates for cDNA synthesis. PrimeScript Reverse Transcriptase (TaKaRa Bio) originating from Moloney Murine Leukemia Virus was used to synthesize the first-strand cDNA from denatured RNA using the manufacturer's protocol. RNA for small RNA blot analysis was extracted using TRI Reagent Solution (Ambion). RNA concentrations were measured using a NanoDrop ND 1000 spectrophotometer.

Small RNA blot hybridization

The small RNA samples (15 μg) from Col-0, *se-1*, *hyl1-2*, *abh1-285* and *sta1-1* were mixed with 5 μl of gel loading buffer (Ambion) and resolved on denaturing 15% polyacrylamide gels containing 7.5 M urea. The separated RNA samples were transferred onto a positively charged Amersham Hybond-N^+ nylon membrane

(GE Healthcare) using a Trans-Blot SD Semi-Dry Electrophoretic Transfer Cell (Bio-Rad). γ-^{32}ATP-radiolabeled single-stranded DNA oligonucleotide probes were used for detection of specific miRNAs. Sequences for probes are listed in Supplementary Table S4. Hybridized membranes were exposed to a storage phosphor screen (Amersham Biosciences) for 1–4 days and the screens were scanned using a Storm 860 phosphoimager (Molecular Dynamics).

Expression analysis of miRNA biogenesis genes

Total RNA from 12-day-old seedlings of WT or *sta1-1* was isolated using Qiagen RNeasy Plant mini kit. The reverse transcription PCR (RT-PCR) was carried out with 50 ng of total RNA using HiPureoneStep RT-PCR kit (GENEPOLE). The RT-PCR programs used were as follows: reverse transcription at 45°C for 10 min, activation of DNA polymerase at 95°C for 2 min, followed by 29 cycles of denaturation at 95°C for 10 s, annealing at 55°C for 10 s and extension at 72°C for 30 s. The gene-specific primers are listed in Supplementary Table S5. All experiments were performed at least three times using seedlings grown independently. The expression level of *UBQ10* was used for loading control.

Quantitative real-time PCR

Quantitative real-time PCR (qRT-PCR) was carried out using DyNAmo Flash SYBR Green qRT-PCR Kit (Finnzymes) in a RotorGene Q RT-PCR cycler (Qiagen). In each 0.1 ml qRT-PCR strip tube (Qiagen), 3 µl cDNA were mixed with 10 µl DyNAmo Flash SYBR Green master mix, 5 µl of Milli-Q H_2O and 1 µl of gene-specific forward and reverse primer for a total volume of 20 µl. Gene-specific primers for miRNA biogenesis genes, miRNA target genes and pri-miRNAs are listed in Supplementary Tables S5, S6 and S7, respectively. Actin2 (At3g18780) or UBQ10 (At4g05320) was used as a reference gene using the primers 5′-GCACCCTGTTCT TCTTACCG-3′/5′-AACCCTCGTAGATTGGCACA-3′ (Actin2) and 5′-GATCTTTGCCGGAAAACAATTGGA GGATGG-3′/5′-CGACTTGTCATTAGAAAGAAAGA GATAACAGG-3′ (UBQ10). The following thermal cycle program was used for all amplifications: 95°C for 7 min; 35 cycles of 95°C for 15 s, 55°C for 20 s, 72°C for 25 s with a gradual 1°C rise per cycle from 72°C to 95°C. Fluorescence of the SYBR Green I dye was measured at the end of the extension step of every PCR cycle. The $\Delta\Delta C_t$ method (36) was used to calculate the normalized gene expression levels of the mutant lines relative to Col-0. The difference in the cycle threshold (C_t) values (ΔC_t) between the mutants and the WT was found for each gene by subtracting the C_t values of the mutants, respectively, from the C_t value of WT. Fold-change values of the target genes were subsequently normalized by dividing the ΔC_t values with the ΔC_t values of the reference gene. Each experiment was carried out at least three times and the mean and standard deviation were calculated.

Amplification of cDNA using intron-spanning pri-miRNA-specific primers

PCR was carried out using HotMasterTaq DNA Polymerase (5 Prime) in a PTC-240 Peltier Thermal Cycler (Bio-Rad). An amount of 20 µl of cDNA was diluted to a volume of 60 µl with nuclease-free H_2O. In each reaction, 2 µl cDNAs were mixed with 1 µl dNTP mix (2.5 mM of each nucleotide), 2 µl 10× HotMasterTaq Buffer (25 mM Mg^{2+}), 0.3 µl HotMasterTaq DNA Polymerase and 1 µl of gene-specific forward and reverse primer (Supplementary Table S8). Milli-Q H_2O was added to make up the reaction volume to 20 µl. β-Tubulin 8 (At5g23860) cDNA was amplified as an internal control using 5′-ATAACCGTTTCAAATTCTCTCTCC-3′ and 5′-TGCAAATCGTTCTCTCCTTG-3′ as forward and reverse primers, respectively. The following thermal cycles were used for all cDNA amplifications: 94°C for 2 min; 30 cycles of 94°C for 30 s, 55°C for 30 s, 72°C for 1.5 min; 72°C for 5 min.

Cloning and sequencing of the amplified fragments of the pri-miRNA transcripts

PCR fragments amplified with primers for pri-miR172b (Supplementary Table S8) were purified with MEGAquick-spin (iNtRON), subcloned into pGEM-easy TA vector (Invitrogen) and transformed to TOP10 competent cells (Invitrogen). The cloned fragments were analyzed by sequencing and aligned with annotated sequences of pri-miRNA172b (www .arabidopsis.org).

Deep sequencing and analysis of small RNA libraries

Small RNA libraries from the *sta1-1* mutant and Col-RD29A-LUC were constructed according to an established protocol (9). Briefly, the 18–30 nt fraction of the small RNAs was separated by resolving total RNA in a 15% denaturing polyacrylamide gel. After sequentially adding 3′- and 5′-adaptors, ligation products were purified and amplified using RT-PCR. PCR products were sequenced using the Illumina Genome Analyzer II.

In-house Perl scripts were used to generate clean reads from raw small RNA sequences by removing 3′-adaptor sequences. Clean reads that were at least 18 nt in length were retained and clustered into unique reads. Only reads with a perfect match to the *Arabidopsis* genome sequence (TAIR9) were used for subsequent analysis. Clean reads were identified as known mature miRNAs if they were identical to the annotated *Arabidopsis* mature miRNAs in the miRBase (release 17) (37). Expression levels of miRNAs [transcripts per 10 million (TPTM)] were calculated by normalizing miRNA counts with the total number of mapped clean reads in the corresponding small RNA library.

Expression analysis with whole-genome tiling array

Arabidopsis Col-RD29A-LUC and *sta1-1* mutant seedlings were grown for 2 weeks on MS agar plates supplemented with 3% sucrose and with daily cycles of 16 h of light at 22°C and 8 h of dark at 18°C. The seedlings were

subjected to cold stress for 24 h at 4°C. Total RNA was isolated from cold-stressed seedlings using the RNeasy plant mini kit (Qiagen). DNA contamination in RNA samples was eliminated by DNase digestion (Qiagen). RNA concentration was quantified with a Nanodrop spectrophotometer at 260 nm. RNA integrity was determined on a Bioanalyzer (Agilent Technology). Whole transcript targets for TILING array hybridization were prepared by using the GeneChip® Whole Transcript Double-Stranded cDNA Synthesis Kit and the GeneChip® Whole Transcript Double-Stranded DNA Terminal Labeling Kit (Affymetrix). Targets were hybridized to GeneChip® *Arabidopsis* Tiling 1.0 R Array (Affymetrix).

To analyze the tiling array data, we re-mapped the tiling array probes to the *Arabidopsis* genome (TAIR9) using SOAP2 (38) and retained only probes that perfectly matched to a unique position in the genome for subsequent analyses. We created a custom chip definition file using the probe mapping result and used the aroma affymetrix framework (39) for quantile normalization of tiling array data.

To identify retained introns, we first calculated the $\log_2$ signal intensity for each annotated intron (TAIR9) based on the trimmed mean of signal intensities from all probes that were mapped to the intron. Introns with less than three mapped probes or low expression ($\log_2$-expression value was <5 in all samples) were removed from further consideration. We used the SAM algorithm (40) to identify introns that showed significantly elevated expression in the *sta1-1* mutant samples than in the WT control samples. A false discovery rate of 0.05 was used as the significance cutoff.

To identify genes that were differentially expressed in the *sta1-1* mutant versus WT, we first used the genefilter package in Bioconductor (http://www.bioconductor.org/) to remove genes that showed low expression level (normalized signal intensity was <100 in all samples) and genes that showed little change in gene expression across samples (interquartile range of $\log_2$ intensities was <0.5). We then applied the linear model method implemented in the *limma* package in Bioconductor to identify genes that showed differential expression. The Benjamini and Hochberg method (41) was used for adjustment for multiple comparisons.

RESULTS

sta1-1 affects pre-mRNA splicing at the whole genome level

We previously showed that unspliced *COR15A* transcript accumulates in *sta1-1* and suggested that *STA1* functions in pre-mRNA splicing (34). However, the genome-wide effect of *sta1-1* on intron-retention was not fully examined. To investigate the global effect of *STA1* on pre-mRNA splicing, we compared the genome-wide expression profiles of *sta1-1* plants with that of WT plants using *Arabidopsis* Tiling Array 1.0 R. As the previously reported unspliced gene was cold-inducible *COR15A*, cold-treated seedlings were used for total RNA extraction. We measured the expression levels of each intron that contains at least three unique probes and found that 695 introns had a significantly higher expression in *sta1-1* than in Col-RD29A-LUC (Supplementary Table S1), indicating that they were not spliced properly in *sta1-1*. This list includes the first intron in the *COR15A* transcript as expected from our published result (34). Among 695 retained introns, 295 (42%) were the first intron and 104 (15%) were the second intron, indicating that similar to *CBC* and *SE* (31), *STA1* has significant effect on splicing at the 5′-end of the transcripts. These results confirm our previous conclusion that *STA1* functions in pre-mRNA splicing. In addition, we identified 2079 genes that were differentially expressed (899 upregulated and 1180 downregulated) in *sta1-1* compared with Col-RD29A-LUC (Supplementary Table S2).

Phenotypes of *sta1-1* are reminiscent of miRNA biogenesis mutants

Bezerra *et al.* (42) suggested that *SE* and *CBC* might function via a common mechanism for mRNA metabolism because the leaf phenotypes of *se-1* were particularly reminiscent of *abh1*/*cbp80* or *cbp20*. Indeed, the similar leaf phenotypes in these mutants were an important clue in finding the dual roles of *SE* and *CBC* for pre-mRNA and pri-miRNA splicing (31). Kim *et al.* (33) also initiated their study on *ABH1*/*CBP80* and *CBP20* based on the leaf phenotype similarity.

We noticed that some of the phenotypes of *sta1-1* resembled those of the miRNA biogenesis mutants, *se-1*, *hyl1-2* and *ago1-25*. Size, shape and vein patterning of leaves are highly regulated by several miRNAs, and therefore defects in miRNA biogenesis pathways may be easily observed by the leaf phenotype (42). Indeed, among the distinct phenotypes in *se-1* are serrated leaves. The leaves of *sta1-1* were also serrated but with a slightly different pattern from *se-1*. The degree of serration in *sta1-1* is not as strong as in *se-1*, and *sta1-1* leaves started to show serration at about the fifth to sixth leaves, while *se-1* developed serrated leaves as early as the third leaf (Figure 1A). In WT, siliques were arranged in a spiral pattern. *ago1-25*, a weak *ago1* allele defective in miRNA biogenesis, often showed an altered silique arrangement (Figure 1B). The abnormal phyllotactic arrangements were also observed in *sta1-1* and *se-1*. Furthermore, the siliques were shorter in *sta1-1*, *se-1* and *hyl1-2* than in WT. The shaping and development of lateral organs are determined by several miRNAs. Therefore, the morphological variations strongly implied general defects of miRNA functions in *sta1-1*.

sta1-1 impairs the accumulation of mature miRNAs

The phenotypic resemblances among *sta1-1*, *se-1*, *hyl1-2* and *abh1*/*cbp80* led us to investigate the levels of miRNAs in *sta1-1*. Using the Illumina platform, we generated 20.4 and 28.0 million clean reads that perfectly matched the *Arabidopsis* genome from the small RNA populations in *sta1-1* and WT, respectively. We compared the normalized counts of mature miRNAs in *sta1-1* and WT and found that the majority of miRNAs had lower expression in *sta1-1* (Supplementary Table S3). Within 79 miRNAs

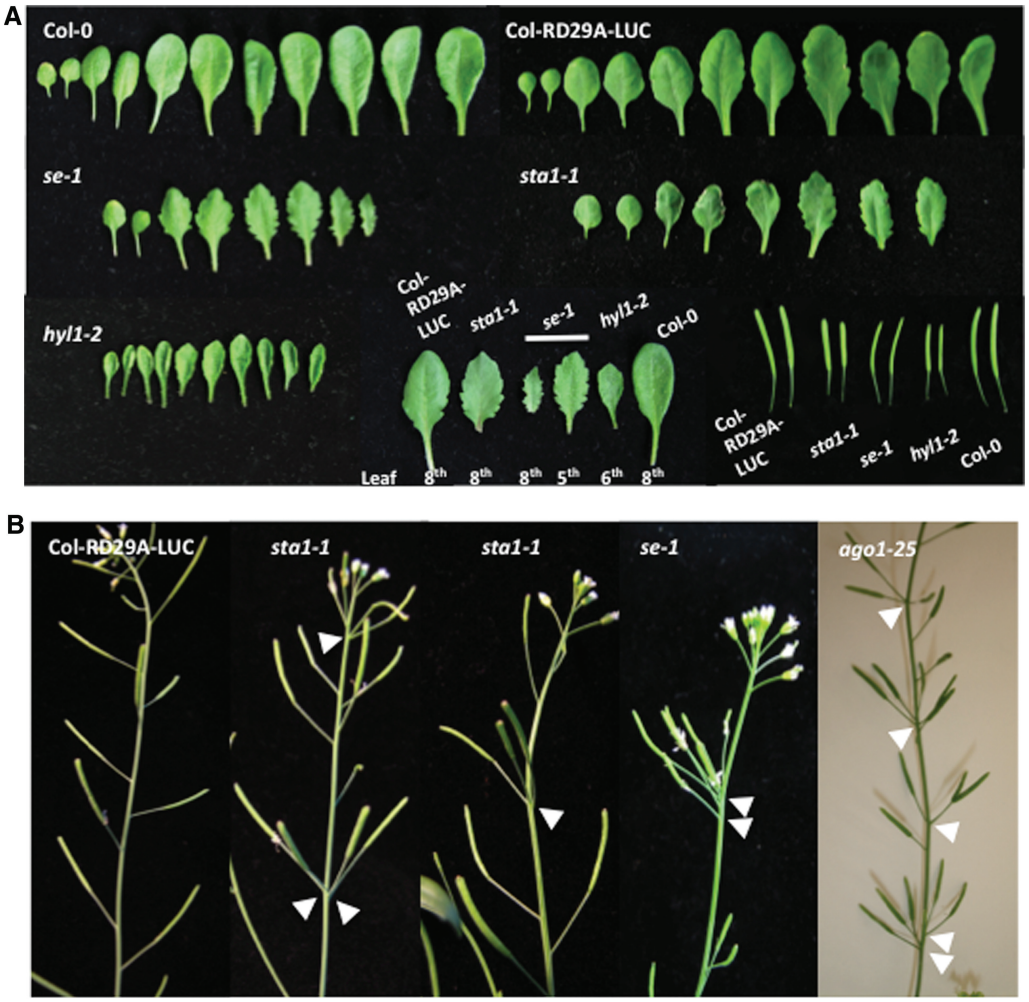

Figure 1. Phenotype comparisons between *sta1-1* and miRNA biogenesis defective mutants. (**A**) Leaf and silique morphology. *sta1-1* showed serrated leaves and small siliques similar to miRNA biogenesis mutants. (**B**) Silique phyllotaxy defects in *sta1-1* and miRNA biogenesis mutants. Arrow heads indicate altered silique phyllotaxy.

that had total expression of at least 20 TPTM, 69 (85%) miRNAs showed reduced expression in *sta1-1*, including 60 (79%) miRNAs whose expression was reduced to 60% or lower compared with WT (Supplementary Table S3). We randomly chose several miRNAs to validate their altered expression in *sta1-1* through small RNA blot hybridization analysis. The accumulation levels of miR156, miR157, miR158, miR159, miR160, miR162, miR166, miR168, miR171, miR172, miR173, miR393, miR398 and miR447 were reduced in *sta1-1* compared with WT (Figure 2 and Supplementary Figure S2). These results were largely consistent with the results of Illumina sequencing (Figure 2, Supplementary Figure S2 and Supplementary Table S3). The only difference between the small RNA blot hybridization and Illumina sequencing was the level of miR164; the expression of miR164 was slightly increased in the *sta1-1* sequencing results, but slightly decreased in the small RNA blot hybridization. Similar levels of reduction in tested miRNAs were also observed in *se-1* and *hyl1-2* except for miR162, miR168 and miR172 levels in *se-1*.

An mRNA cap-binding protein, ABH1/CBP80 was shown to act in pri-miRNA processing (31). The leaf and phyllotaxy phenotypes described above were also found in *abh1*/*cbp80* mutants (Supplementary Figure S1). Small RNA blot hybridization analysis showed that the miRNA reductions in *sta1-1* were more significant than those in *abh1*/*cbp80* (Supplementary Figure S2). It should be noted that Col-0 was mostly used as a WT control throughout our experiments except for the tiling array and small RNA sequencing in which Col-RD29A-LUC was used as a control. *sta1-1* was originally isolated from Columbia-*gl1* harboring the stress-responsive RD29A promoter-driven luciferase (Col-RD29A-LUC) (34). Recent reports showed that different accumulation patterns of miRNAs can be observed in different *Arabidopsis* accessions (43). Thus, some selected miRNA accumulation levels were compared between Col-0 and Col-RD29A-LUC and very similar levels of miR156, miR158, miR159, miR160, miR166 and miR172 accumulation were observed (Supplementary Figure S3). In addition, the patterns of higher

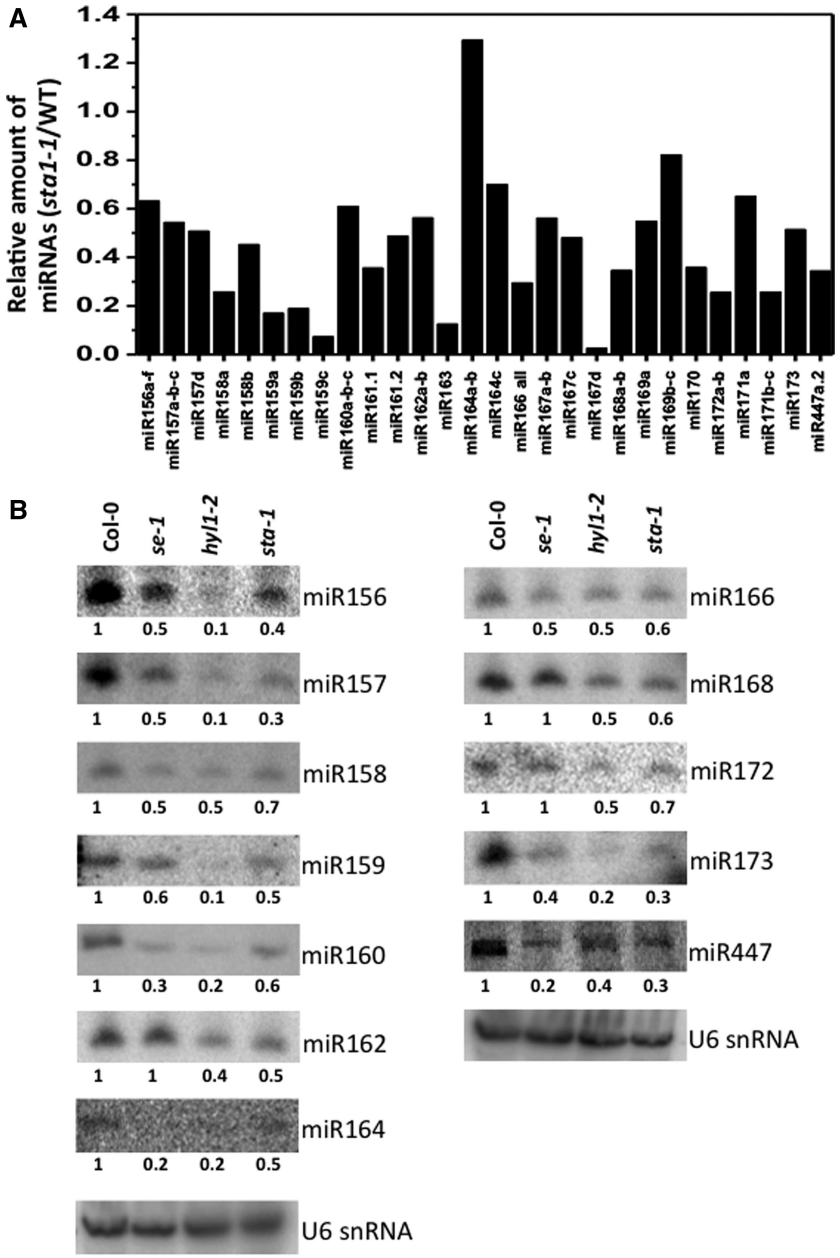

Figure 2. Reduction of miRNA levels in *sta1-1*. (**A**) Small RNA sequencing analysis of miRNAs in WT and *sta1-1*. From the small RNA sequencing results, abundance of miRNAs in *sta1-1* was compared with WT. (**B**) RNA blot hybridization of miRNAs from 4-week-old Col-0, *se-1*, *hyl1-2* and *sta1-1*. The levels of U6 small nuclear RNA were shown as loading controls. Numbers below the blot images are relative intensities of the miRNA bands.

accumulation of pri-miRNAs in *sta1-1* were still observed when compared with its background line, Col-RD29A-LUC (Supplementary Figure S4). Taken together, these results suggest that *STA1* is involved in miRNA biogenesis.

Expression levels of miRNA target genes are increased in *sta1-1*

Each miRNA recognizes specific mRNA target(s) through sequence specificity and initiates degradation/translation repression of the targets (44–46). Since the amount of target mRNAs is highly inversely correlated to the amount of specific miRNAs, we determined the levels of target mRNAs for some miRNAs by qRT-PCR (Figure 3). *SQUAMOSA PROMOTER-BINDING PROTEIN-LIKE* (*SPL*) transcription factors are involved in a variety of developmental processes in flowers and leaves and the expression of the *SPL* gene family is directly regulated by miR156/157 (47–49). The upregulation of target *SPL3* transcripts was expected due to the decrease of miR156 and miR157 in *sta1-1* (Figure 2). As expected, an increase of the *SPL3* transcript level was observed in *sta1-1* (Figure 3). Increased *SPL3* expression levels were also observed in the other two miRNA defective mutants

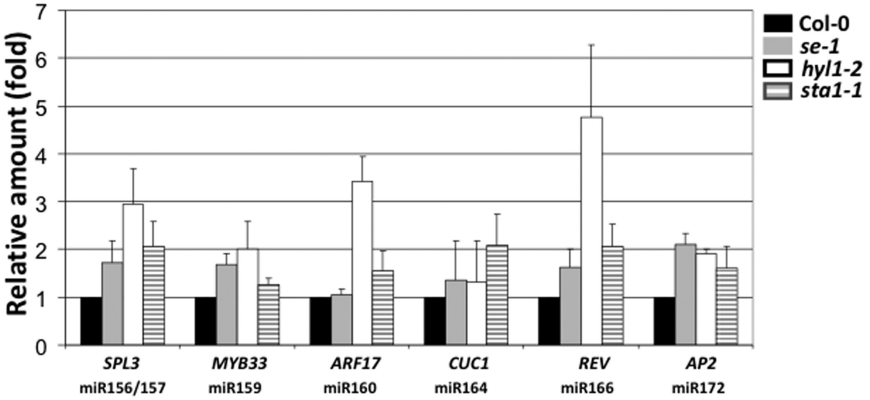

Figure 3. qRT-PCR expression analysis of selected miRNA target transcripts in Col-0, *se-1*, *hyl1-2* and *sta1-1*. Relative amounts of mRNA levels were obtained by dividing the expression level of the mutant with WT value. Three biological samples were used.

as these mutants also generated lower levels of miR156/157 than WT (Figure 3). Plastochron, a temporal period between two successive leaves (50), is modulated by the transcript levels of *SPL9/15* and eventually determines the leaf numbers at bolting (51). High levels of *SPL9/15* can cause long plastochron and decreased leaf numbers at bolting. Indeed, in the miRNA biogenesis mutants examined, the reduced miR156/157 levels were linked to the higher expression levels of *SPL9/15* genes and eventually the decreased leaf number (Supplementary Figure S5). Interestingly, the levels of *SPL9* transcripts show a stronger correlation than those of *SPL15* transcripts to the leaf numbers in the tested mutants. *MYB33* encodes a MYB protein-like transcription factor that regulates many developmental processes, and the expression of *MYB33* is regulated by miRNA159 (52). *se-1*, *hyl1-2* and *sta1-1* with decreased miR159 levels showed marginally increased expression levels of *MYB33* (Figure 3). *AUXIN RESPONSE FACTOR17* (*ARF17*), whose expression is controlled by miR160, is important for proper development and modulates expression of early auxin response genes (53). Higher levels of *ARF17* transcripts accumulated in *sta1-1*, consistent with its reduced miR160 levels compared with WT (Figure 3). *CUP-SHAPED COTYLEDON1* (*CUC1*) is essential for boundary size control of meristems and is a target of miR164 (54). *REVOLUTA* (*REV*), the target of miR166, is expressed in young leaves and controls development of the leaves (55). Compared with WT, the accumulation of *CUC1* and *REV* transcripts was higher in *sta1-1*, which is linked to decreased miR164/166 levels and explains the serrated leaf phenotype of *sta1-1* (Figure 3). *APETALA 2* (*AP2*), a target of miR172 (56), showed a slight increase in *se-1*, *hyl1-2* and *sta1-1* that accumulated lower amounts of miR172 than WT (Figure 3). Overall, the expression levels of target mRNAs in *se-1*, *hyl1-2* and *sta1-1* were largely inverse-correlated to the corresponding miRNA levels in each mutant (Figures 2 and 3).

Expression levels of a subset of pri-miRNAs are increased in *sta1-1*

The results of small RNA blot hybridization analysis (Figure 2) suggested a possible role of *STA1* in miRNA biogenesis. Mutations in *HYL1* and *SE* generally lead to a dramatic increase in accumulation of pri-miRNAs (19,21). To investigate the involvement of *STA1* in the pri-miRNA processing, we determined pri-miRNA transcript levels by qRT-PCR (Figure 4). Transcripts of all tested pri-miRNAs accumulated more in *sta1-1* compared with WT. Consistent with the previous reports, most transcript levels of tested pri-miRNAs were largely increased in *se-1* and *hyl1-2*. These data indicate that *STA1* is a factor required for proper processing of pri-miRNAs.

sta1-1 accumulates unspliced transcript of pri-miRNAs

Recent studies showed that several pri-miRNAs contain introns (31,56–58). In the case of intron-containing pri-miRNAs, the miRNA biogenesis pathway can be categorized into two distinct steps: (i) splicing of intron-containing pri-miRNAs and (ii) processing of pri-miRNAs into pre-miRNAs and eventually mature miRNAs. *SE* has roles in splicing of introns in several pri-miRNAs and also in further steps of miRNA biogenesis from the intron-less and intron-excised pri-miRNAs (31). The STA1 protein has high similarity to human U5 snRNP-associated 102-kDa protein, PRP1p and Prp6p (34). Indeed, pre-mRNA splicing of a stress-responsive *COR15A* gene was defective in the *sta1-1* mutants (34), and the tiling array results from this study confirmed the general role of *STA1* in the splicing process (Supplementary Table S1). Based on these results, we investigated the plausible roles of *STA1* in splicing of pri-miRNAs. Five intron-containing pri-miRNAs were selected for the splicing analysis by RT-PCR; pri-miR160a (one intron), pri-miR166a (one intron), pri-miR166b (two introns), pri-miR172a (two introns) and pri-miR172b (three introns). We compared the splicing variants of the pri-miRNAs from Col-0, *hyl1-2*, *se-1* and *sta1-1*. Splicing variants were examined more than eight times with four different biological samples and the tests consistently produced the similar results. The unspliced pri-miR160a (~2.0 kb) accumulated more in *se-1* and *sta1-1* compared with Col-0 and *hyl1-2* (Figure 5A). The *se-1* and *hyl1-2* mutants displayed a band ~850 bp which corresponds to the predicted size of mature pri-miR160a, while both Col-0 and *sta1-1* did

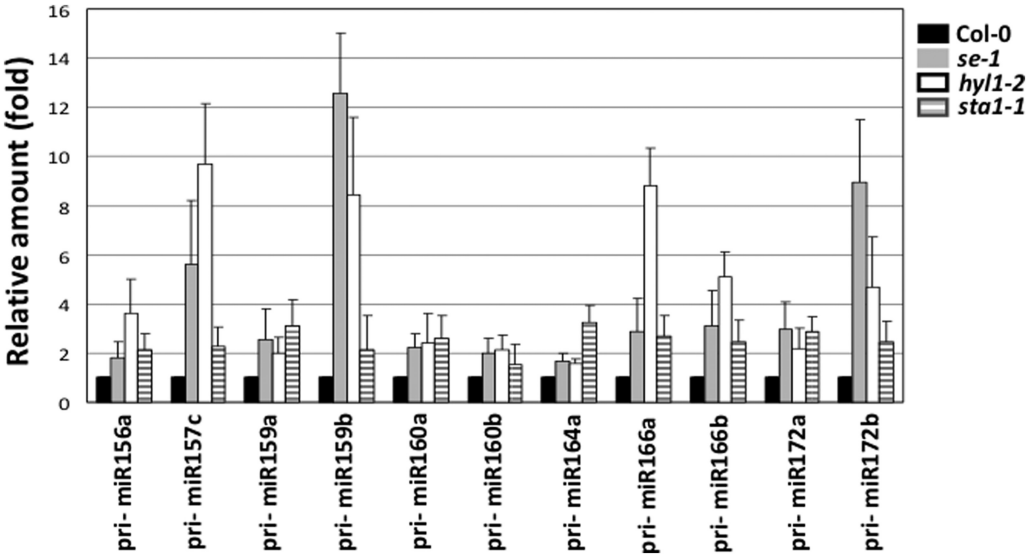

Figure 4. qRT-PCR expression analysis of selected pri-miRNA transcripts in Col-0, *se-1, hyl1-2 and sta1-1*. Relative amounts of mRNA levels were obtained by dividing the expression level of the mutant with the WT value. Three biological samples were used.

not show this band. The accumulation of unspliced pri-miR160a transcripts without mature pri-miR160a fragment in *sta1-1* implies the roles of STA1 in splicing of pri-miR160a. The other bands around 1.5 kb and 650 bp in *se-1* and *hyl1-2* and 750 bp in Col-0 may be the products of mis-splicing. High levels of unspliced pri-miRNA166a transcripts accumulated in *se-1*, *hyl1-2* and *sta1-1* as compared with Col-0, indicating the similar impairment in pri-miR166a splicing process in these mutants (Figure 5B). Unlike *sta1-1*, *se-1* and *hyl1-2* showed two additional fragments with sizes of ~650 and ~1000 bp. The former matches to the predicted size of mature pri-miR166a and the latter might be the products of alternative splicing (Figure 5B). Similar to pri-miR166a, unspliced pri-miR166b was accumulated more in *se-1*, *hyl1-2* and *sta1-1* than in Col-0 (Figure 5C). In contrast to a previous report (57), we could not observe the spliced fragments of pri-miR166 in *hyl1-2*. We suspect that the splicing efficiency of intron containing pri-miRNAs may be more dependent on growth conditions or developmental stages in *hyl1-2* than other mutants. Nascent transcript of pri-miR172a (Figure 5D) with the predicted size of 2 kb contains two introns. As shown in Figure 5D, unspliced pri-miRNA172a was accumulated more in *sta1-1* than in Col-0. The splicing-intermediate transcript with one intron (148 bp) and mature pri-miR172a were clearly observed in *se-1* and *hyl1-2*, but not in WT and *sta1-1*. The missing bands of the splicing-intermediates and fully spliced pri-miR172a in WT and *sta1-1* might result from different reasons; in WT, the spliced pri-miR172a could be quickly used for further downstream steps while in *sta1-1*, the splicing of pri-miRNA172a was inhibited from the beginning. In fact, the missing band of 850 bp (fully spliced pri-miR160a) in pri-miR160a and of ~650 bp in pri-miR166a in both Col-0 and *sta1-1* (Figure 5A) can be explained in the same way. These results suggest that STA1 functions at very early steps in pri-miRNA processing. Unspliced pri-miR172b (Figure 5E) contains three introns with the total size of ~1.5 kb and mature pri-miR172b was predicted to be ~0.7 kb. Higher accumulation of unspliced pri-miR172b was also observed in *sta1-1* compared with Col-0, *se-1* and *hyl1-2*. In addition to the intron retention in *sta1-1*, we observed unusual accumulation of the predicted mature pri-miR172b (~0.7 kb), which was present in Col-0, *se-1* and *hyl1-2* at very similar levels (Figure 5E). Normally, mature pri-miRNAs rapidly undergo further processing to pre-miRNAs that are known to be less detectable in WT than the processing defective mutants (59). To clarify the identity of the ~0.7-kb fragment in Col-0, we cloned the fragment for sequence analysis and found that the fragment is a mis-spliced product caused by an exon-skipping at 5′-region during splicing (Figure 5B). The sequence analysis also found that the ~0.7 kb fragment from *hyl1-2* was normally spliced mature pri-miR172b but the fragment from *se-1* was not. Furthermore, several bands ranging from ~0.85 to ~1.4 kb accumulated to high levels in *se-1* and *hyl1-2*, but not in Col-0 and *sta1-1* (Figure 5E). Interestingly, the splicing intermediates of pri-miR172b were more variable in *hyl1-2* than in *se-1*. Indeed, the sequence analysis of these fragments showed various intermediates in *hyl1-2* and only one kind of intermediate in *se-1* (Figure 5B). This may be due to the involvement of *SE* in the splicing process in addition to the miRNA processing pathway (31). The other bands of ~1.2 kb (the second band from the top) and ~0.7 kb (the last band from the top) in *se-1* and weak bands (the second, third and fifth from the top) in *hyl1-2* could not be retrieved for sequence analysis. Apparent unspliced nascent pri-miR172b transcript in sta*1-1* was confirmed by the sequence analysis. Thus, the observation that *stat1-1* accumulated non-spliced nascent pri-miR172b without any splicing

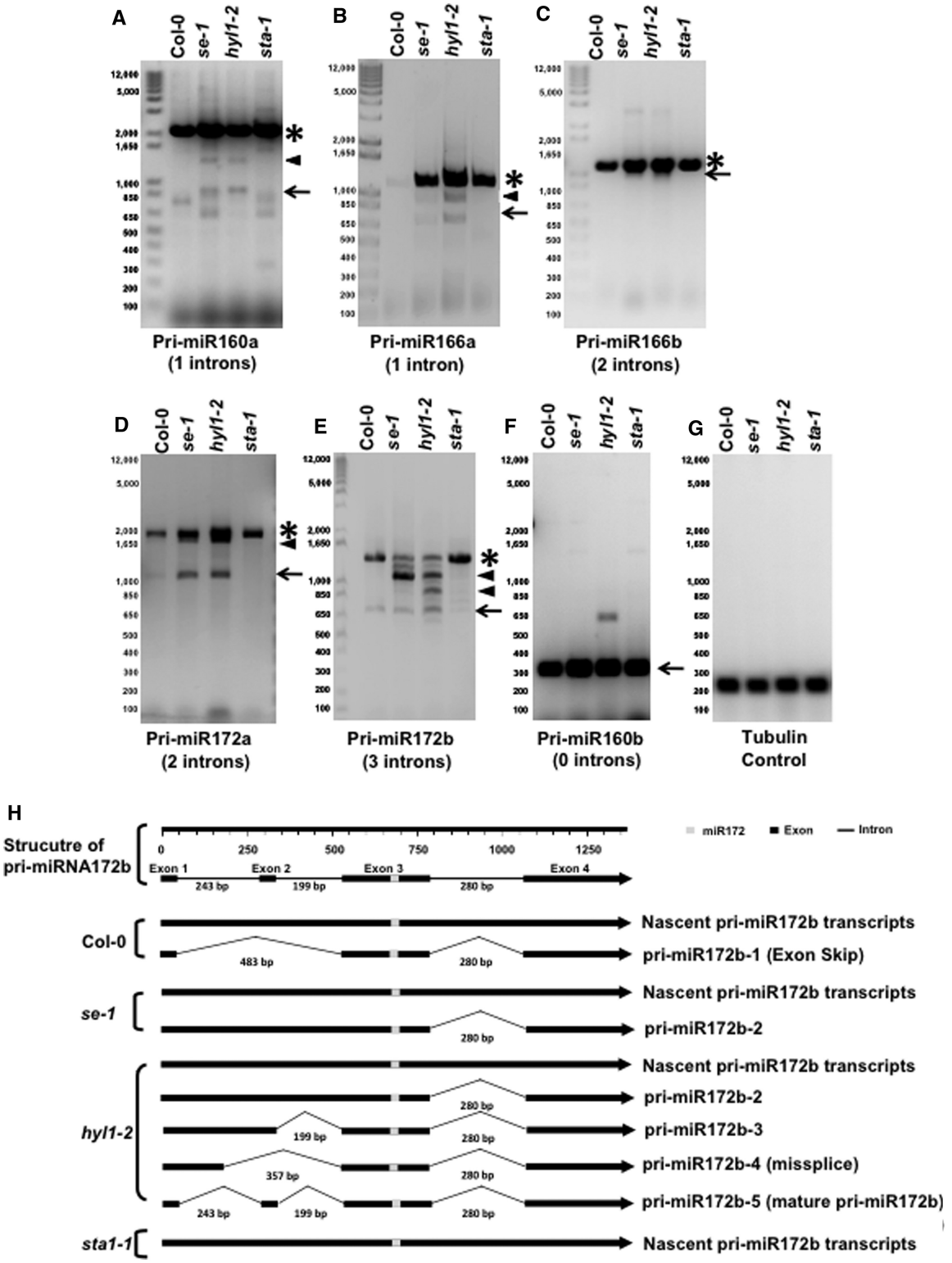

Figure 5. Intron-retention analysis of selected pri-miRNA. (**A**–**G**) Analysis of retained intron in Col-0, *se-1, hyl1-2 and sta1-1*. Five intron-containing pri-miRNAs were investigated by RT-PCR. Splicing pattern of pri-miR160b (A), pri-miR166a (B), pri-miR166b (C), pri-miR172a (D), pri-miR172b (E) and pri-miR166a (F). Tubulin gene was used as a loading control (G). Asterisk, unspliced pri-miRNA; arrow-head, splicing intermediate; arrow, fully spliced or mature pri-miRNA. (**H**) Patterns of processing intermediates of pri-miR172b in Col-0, *se-1, hyl1-2 and sta1-1*. RT-PCR fragments of pri-miR172b in each genotype were cloned and sequenced to compare the retention patterns.

variants implies that STA1 has a major role in pri-miRNA splicing. In fact, of all tested pri-miRNAs, accumulation of apparent splicing intermediates or misspliced transcripts was observed in *se-1* and *hyl1-2,* but not in *sta1-1* (Figure 5), strongly suggesting a significant role of *STA1* in pri-miRNA splicing steps, rather than in the cleavage of pri-miRNAs into mature miRNAs. We also quantitatively evaluate the retention of introns in pri-miR172b by comparing the levels of the introns in the WT control and *sta1-1* using qRT-PCR. The retention levels of intron 1 and 2 in pri-miR172b were higher in *se-1*, *hyl1-2* and *sta1-1* than Col-0, while the retention of intron 3 was high only in *sta1-1* (Supplementary Figure S6). These results are consistent with the results from RT-PCR (Figure 5E) where the major bands were the unspliced transcript (for *sta1-1*) and the splicing intermediate without the third intron (for *se-1* and *hyl1-2*). Overall, the results indicate that *sta1-1* causes high levels of intron retention and accumulates unspliced transcript of pri-miRNAs.

DCL1 transcript levels were reduced in *sta1-1*

Intriguingly, the intron-less pri-miR160b transcripts were accumulated slightly more in *sta1-1* than in Col-0, which was similar to those in *se-1* and *hyl1-2* (Figure 5F). Indeed, many intronless miRNAs accumulated less in *sta1-1* than in WT in our small RNA sequencing results (Supplementary Table S3). Therefore, we examined the transcript levels of canonical miRNA biogenesis genes including *DCL1*, *HYL1*, *SE*, *HEN1* and *HST1* and found the transcript level of *DCL1* is reduced in *sta1-1* (Figure 6A). The decreased levels of *DCL1* transcript in *sta1-1* were confirmed by qRT-PCR (Figure 6B). We speculate that *STA1* involvement in miRNA processing of intronless miRNA transcripts could be mediated at least in part by modulating the levels of *DCL1* transcripts.

DISCUSSION

Recently, three research groups independently reported an important relationship between pre-mRNA maturation and pri-miRNA processing. Laubinger *et al.* (31) revealed the dual roles of *ABH1*/*CBP80, CBP20* and *SE* in pre-mRNA splicing and pri-miRNA processing. Gregory *et al.* (60) also uncovered the function of *ABH1*/*CBP*80 in miRNA biogenesis. Around the same time, Kim *et al.* (33) showed that ABH1/CBP80 and CBP20 directly bind to pri-miRNA transcripts and have a general role in miRNA biogenesis, but other reported cap-binding proteins in plants such as CUM1 (eIF4E1) and CUM2 (eIF4G) are irrelevant (33). Compared with the canonical miRNA processing components (DCL1, SE, HYL1, etc.), CBC seems to play less essential roles in the miRNA processing pathway because most miRNAs were not significantly affected by *ABH1*/*CBP80* and *CBP20* deficiency (Supplementary Figure 2) (61). However, the additional role of CBC in miRNA biogenesis introduced a new prospect on the proteins that play roles in mRNA metabolism; cap-binding, splicing and polyadenylation can influence miRNA processing pathway. Several studies reported that some of pri-miRNA transcripts appear to be spliced, polyadenylated and capped, which implies splicing may also be an important step for further processing (56,58,62). Hence, two fundamental questions arise: how does *ABH1*/*CBP80* or the cap-binding process affect miRNA biogenesis and are splicing and polyadenylation of pri-miRNAs also important for miRNA biogenesis? For the former question, it was suggested that ABH1/CBP80 guides mature pri-miRNAs to the miRNA processing complex by direct interaction with miRNA processing proteins (63). For the latter question, analysis of reported mutants defective in general splicing or polyadenylation could be a plausible approach. In addition, as the results from the *se* mutant suggested (31), examination of miRNA biogenesis gene involvement in splicing would answer how important the splicing is in miRNA biogenesis. To answer this question, Szarzynska *et al.* (57) performed a detailed study on *HYL1*-dependent processing of intron-containing pri-miRNAs and suggested the coupled roles of *HYL1* in splicing and miRNA processing. In our results, the accumulation of unspliced pri-miR166a, pri-miR166b and pri-miR172a was observed in *hyl1-2*, which supports the possible role of *HYL1* in pri-miRNA splicing (Figure 5). However, the splicing of pri-miR160a and pri-miR172b transcripts was not dramatically affected in *hyl1-2* and fully spliced pri-miRNAs were detected in all tested pri-miRNAs in *hyl1-2*. In addition, various splicing intermediates of pri-miRNAs were highly accumulated in *hyl1-2* (Figure 5). It should be noted that the splicing intermediates or abnormally spliced transcripts were more often found in *hyl1-2* than in *se-1*. This means that defects in SE-dependent splicing might block post-splicing processes, resulting in lower accumulation of splicing variants in *se-1* compared with *hyl1-2*. Thus, these results suggest that *SE* appears to be more important for splicing than *HYL1*. Although our data did not fully address whether *HYL1* functions simultaneously in the splicing and miRNA processing steps, our observation of accumulation of the splicing intermediates and mature pri-miRNAs in *hyl1-2* supports the hypothesis that *HYL1* functions primarily or preferentially in the post-splicing processes to produce pre-miRNA and miRNAs and perhaps functions selectively in pri-miRNA splicing. These splicing defects are clearly contrary to the fact that the pri-miRNA splicing defective *sta1-1* mutants did not show any splicing intermediates of tested pri-miRNAs (Figure 5), indicating that *STA1* functions more significantly in pri-miRNA splicing than the other two genes.

Our study with the *sta1-1* mutants defective in an *Arabidopsis* pre-mRNA processing factor 6 homolog showed that splicing is an important step for both pre-mRNA and pri-miRNA processing. The first indication of the dual functions of *STA1* was the phenotype similarity between *sta1-1* and the other miRNA defective mutants. Indeed, we found dramatic reduction in the majority of miRNAs, the accumulation of pri-miRNAs and target mRNAs in *sta1-1* (Figures 2–4 and Supplementary Table S3). Suggested by *STA1* function in pre-mRNA splicing, we tested the possible function of

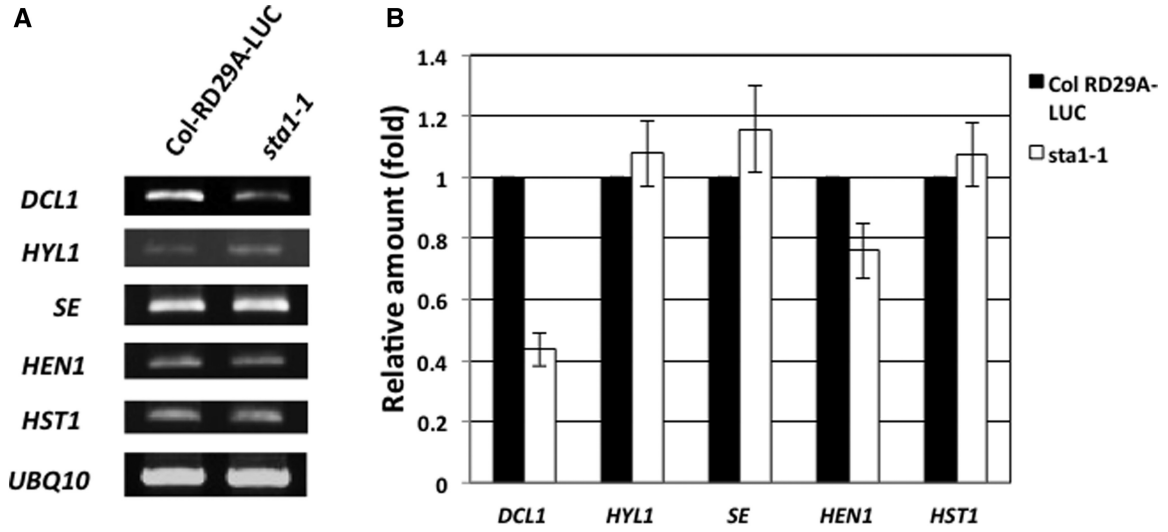

Figure 6. Comparison of transcript levels of miRNA biogenesis genes in Col-RD29A-LUC and *sta1-1*. (**A**) RT-PCR results of miRNA biogenesis genes. *DCL1* transcript levels were lower in *sta1-1* than Col-RD29A-LUC. (**B**) qRT-PCR results of miRNA biogenesis genes. qRT-PCR confirmed that reduced levels of *DCL1* transcript in *sta1-1*. Three replicates were used.

STA1 on pri-miRNA splicing by RT-PCR. Our results showed that *STA1* also has roles in splicing of intron-containing pri-miRNAs (Figure 5). For example, all introns of pri-miR172b are retained in *sta1-1* but not in *se-1* and *hyl1-2* (Figure 5E). Sequencing of cloned fragments showed that the unspliced pri-miR172b in *sta1-1* perfectly matched to the annotated sequence of nascent pri-miR172b transcript. Moreover, accumulation of mature pri-miRNAs was undetectable in *sta1-1*. These different patterns of pri-miRNA processing intermediates in these mutants also suggest that *STA1* has distinct functions from the other genes—particularly *SE* in splicing of pri-miRNAs. While *HYL1* and *SE* have canonical roles in miRNA processing with their potential roles in splicing, *STA1* seems to have major roles in splicing of nascent pri-miRNA transcripts. Furthermore, *STA1*-dependent splicing seems more important for further downstream processing than *ABH1*/*CBP80* because *sta1-1* showed more significantly reduced levels of many miRNAs than *abh1*/*cbp80* (Supplementary Figure S2). Previously, Yang *et al.* (22) reported that *hyl1-1 se-1* double mutants are embryonic lethal. Similarly, a homozygous T-DNA insertion (SALK _009304) in *STA1* likely causes the embryonic lethality which also implies the vital roles of *STA1* in pri-miRNA splicing and also pre-mRNA splicing for gene expression control from the early stage of development (34).

Our data also showed that the accumulation of intronless pri-miR160b in *sta1-1* was slightly higher than control plants (Figure 5). In addition, small RNA sequencing results indicated the general reduction of mature miRNAs including those generated from intronless pri-miRNAs. These results cannot be interpreted solely by our suggestion on the roles of *STA1* in the intron-containing pri-miRNA splicing. Interestingly, we found that the level of *DCL1* transcripts was notably reduced in *sta1-1* (Figure 6). This reduction of *DCL1* transcript levels appears to be because of splicing defects in *sta1-1* rather than regulation by miR162. *DCL1* transcripts are constitutively subject to negative feedback regulation by miR162 (64). However, *sta1-1* accumulates miR162 only at half the levels of WT (Figure 2). Thus, reduced *DCL1* levels in *sta1-1* cannot be explained by miR162 regulation. Our RT-PCR results showed reduced levels of spliced *DCL1* transcripts along with an inversely correlated, high accumulation of unspliced *DCL1* transcripts in *sta1-1* (Supplementary Figure S7), suggesting splicing defect-caused downregulation of *DCL1* in *sta1-1*. However, this unspliced *DCL1* transcript band was not always detected in our RT-PCR results. This is also probably because of the unstable nature of unspliced *DCL1* transcripts or rapid degradation of unspliced *DCL1* transcripts by unknown mechanisms rather than miR162-mediated negative regulation. Taken together, these results suggested that *STA1* also functions in processing of intronless pri-miRNA, probably through the modulation of the levels of *DCL1* transcripts (Figure 7). However, this does not weaken our argument that *STA1* has an important role in splicing of intron-containing pri-miRNAs during miRNA biogenesis. Kurihara *et al.* (19) showed that *dcl1-9*, a weak allele of *dcl1*, accumulates fully spliced pri-miR166a (between 1000 and 500 bp), while we observed only unspliced pri-miR166a (>1000 bp) in *sta1-1* where the level of *DCL1* is supposed to be low. These observations indicate that *DCL1* is not involved in pri-miR166a splicing and the accumulation of unspliced pri-miR166a transcript is mainly due to the defects in splicing in *sta1-1*. These findings also suggest that the STA1-dependent splicing is precedent to DCL1-catalyzed miRNA processing pathway. In our analysis, fully spliced pri-miRNAs of all the tested intron-containing pri-miRNAs were not observed in *sta1-1*. In summary, we suggest that *STA1* is a new player in miRNA biogenesis and has a major role in splicing intron-containing pri-miRNAs. *STA1* also seems to have an indirect role in processing intronless

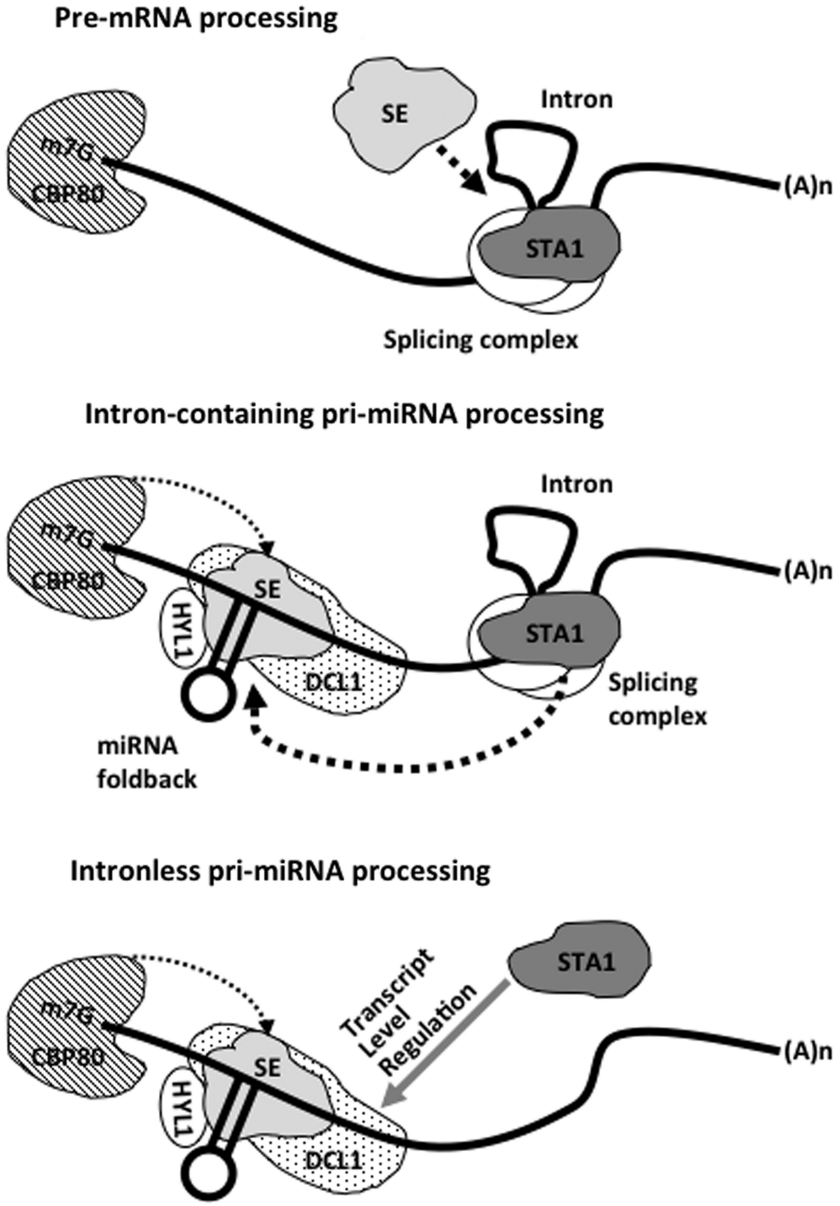

Figure 7. A model for *STA1* function in miRNA biogenesis. *SE* involvement in pre-mRNA processing was previously reported (57). In addition to mRNA splicing, STA1 is also involved in splicing of intron-containing pri-miRNAs. STA1 has a direct role in pri-miRNA splicing that affects miRNA processing and also indirectly affects intronless pri-miRNA processing by modulating the *DCL1* transcript levels. It is not clear that *STA1* regulation on the *DCL1* transcript levels occurs through the STA1-including splicing complex or other *STA1* unique functions.

pri-miRNAs probably through modulating the levels of *DCL1* transcripts (Figure 7).

We further envisage that STA1 may be the part of a large miRNA processing/splicesome complex that orchestrates pri-miRNA splicing and processing. Certainly, further investigations for detailed mechanism are required to understand the molecular linkage between upstream splicing and downstream processing in miRNA biogenesis. For instance, STA1 has domains known for protein–protein interactions that may be important for its interaction with the other components in miRNA biogenesis. DCL1, SE, HYL1 and ABH1/CBP80 will be the primary targets for protein interaction studies of STA1.

SUPPLEMENTARY DATA

Supplementary Data are available at NAR Online: Supplementary Tables 1–8, and Supplementary Figures 1–7.

ACKNOWLEDGEMENTS

The authors thank laboratory members for helpful discussion and Brian Christopher King for helpful comments on the manuscript. S.W.Y. gratefully acknowledges support from Center for Synthetic Biology at University of Copenhagen and experimental equipment support from iNtRON Biotechnology, Inc. Korea.

FUNDING

The National Research Foundation of Korea by the Korean Government MEST [2011-0027376 to B.-h.L., 2012R1A1A2008826 to B.-h.L.]; Next-Generation BioGreen 21 Program, Rural Development Administration, Republic of Korea [PJ009104 to B.-h.L.]; Sogang University Research [201214003.01 to B.-h.L.]; UNIK research initiative of the Danish Ministry of Science, Technology and Innovation [09-065274 to S.W.Y.]; Chinese Academy of Sciences and National Institutes of Health Grants [R01GM070795 to J.-K.Z., R01GM059138 to J.-K.Z.]; USDA Grant [2008-35100-04518 to J.-K.Z.]; University of California at Riverside Initial Complement Fund and a United States Department of Agriculture hatch fund [CA-R-BPS-7754H to R.L.]. Funding for open access charge: National Research Foundation of Korea by the Korean Government MEST [2012R1A1A2008826 to B.-h.L.]

Conflict of interest statement. None declared.

REFERENCES

1. Carrington,J.C. and Ambros,V. (2003) Role of microRNAs in plant and animal development. *Science*, **301**, 336–338.
2. Chen,X.M. (2004) A microRNA as a translational repressor of APETALA2 in *Arabidopsis* flower development. *Science*, **303**, 2022–2025.
3. Lauter,N., Kampani,A., Carlson,S., Goebel,M. and Moose,S.P. (2005) microRNA172 down-regulates glossy15 to promote vegetative phase change in maize. *Proc. Natl Acad. Sci. USA*, **102**, 9412–9417.
4. Reyes,J.L. and Chua,N.H. (2007) ABA induction of miR159 controls transcript levels of two MYB factors during *Arabidopsis* seed germination. *Plant J.*, **49**, 592–606.
5. Bari,R., Pant,B.D., Stitt,M. and Scheible,W.R. (2006) PHO2, microRNA399, and PHR1 define a phosphate-signaling pathway in plants. *Plant Physiol.*, **141**, 988–999.
6. Fujii,H., Chiou,T.J., Lin,S.I., Aung,K. and Zhu,J.K. (2005) A miRNA involved in phosphate-starvation response in *Arabidopsis*. *Curr. Biol.*, **15**, 2038–2043.
7. Hwang,E.W., Shin,S.J., Yu,B.K., Byun,M.O. and Kwon,H.B. (2011) miR171 family members are involved in drought response in *Solanum tuberosum*. *J. Plant Biol.*, **54**, 43–48.
8. Sunkar,R., Li,Y.F. and Jagadeeswaran,G. (2012) Functions of microRNAs in plant stress responses. *Trends Plant Sci.*, **17**, 196–203.
9. Sunkar,R. and Zhu,J.K. (2004) Novel and stress-regulated microRNAs and other small RNAs from *Arabidopsis*. *Plant Cell*, **16**, 2001–2019.
10. Zhao,B.T., Ge,L.F., Liang,R.Q., Li,W., Ruan,K.C., Lin,H.X. and Jin,Y.X. (2009) Members of miR-169 family are induced by high salinity and transiently inhibit the NF-YA transcription factor. *BMC Mol. Biol.*, **10**, 29.
11. Boutet,S., Vazquez,F., Liu,J., Beclin,C., Fagard,M., Gratias,A., Morel,J.B., Crete,P., Chen,X.M. and Vaucheret,H. (2003) *Arabidopsis* HEN1: a genetic link between endogenous miRNA controlling development and siRNA controlling transgene silencing and virus resistance. *Curr. Biol.*, **13**, 843–848.
12. Grigg,S.P., Canales,C., Hay,A. and Tsiantis,M. (2005) SERRATE coordinates shoot meristem function and leaf axial patterning in *Arabidopsis*. *Nature*, **437**, 1022–1026.
13. Lu,C. and Fedoroff,N. (2000) A mutation in the *Arabidopsis* HYL1 gene encoding a dsRNA binding protein affects responses to abscisic acid, auxin, and cytokinin. *Plant Cell*, **12**, 2351–2365.
14. Park,M.Y., Wu,G., Gonzalez-Sulser,A., Vaucheret,H. and Poethig,R.S. (2005) Nuclear processing and export of microRNAs in *Arabidopsis*. *Proc. Natl Acad. Sci. USA*, **102**, 3691–3696.
15. Park,W., Li,J.J., Song,R.T., Messing,J. and Chen,X.M. (2002) CARPEL FACTORY, a Dicer homolog, and HEN1, a novel protein, act in microRNA metabolism in *Arabidopsis* thaliana. *Curr. Biol.*, **12**, 1484–1495.
16. Reinhart,B.J., Weinstein,E.G., Rhoades,M.W., Bartel,B. and Bartel,D.P. (2002) MicroRNAs in plants. *Genes Dev.*, **16**, 1616–1626.
17. Kurihara,Y. and Watanabe,Y. (2004) *Arabidopsis* micro-RNA biogenesis through Dicer-like 1 protein functions. *Proc. Natl Acad. Sci. USA*, **101**, 12753–12758.
18. Dong,Z., Han,M.H. and Fedoroff,N. (2008) The RNA-binding proteins HYL1 and SE promote accurate in vitro processing of pri-miRNA by DCL1. *Proc. Natl Acad. Sci. USA*, **105**, 9970–9975.
19. Kurihara,Y., Takashi,Y. and Watanabe,Y. (2006) The interaction between DCL1 and HYL1 is important for efficient and precise processing of pri-miRNA in plant microRNA biogenesis. *RNA*, **12**, 206–212.
20. Yang,S.W., Chen,H.Y., Yang,J., Machida,S., Chua,N.H. and Yuan,Y.A. (2010) Structure of *Arabidopsis* HYPONASTIC LEAVES1 and its molecular implications for miRNA processing. *Structure*, **18**, 594–605.
21. Lobbes,D., Rallapalli,G., Schmidt,D.D., Martin,C. and Clarke,J. (2006) SERRATE: a new player on the plant microRNA scene. *EMBO Rep.*, **7**, 1052–1058.
22. Yang,L., Liu,Z.Q., Lu,F., Dong,A.W. and Huang,H. (2006) SERRATE is a novel nuclear regulator in primary microRNA processing in *Arabidopsis*. *Plant J.*, **47**, 841–850.
23. Yu,B., Yang,Z.Y., Li,J.J., Minakhina,S., Yang,M.C., Padgett,R.W., Steward,R. and Chen,X.M. (2005) Methylation as a crucial step in plant microRNA biogenesis. *Science*, **307**, 932–935.
24. Yu,B., Bi,L., Zheng,B.L., Ji,L.J., Chevalier,D., Agarwal,M., Ramachandran,V., Li,W.X., Lagrange,T., Walker,J.C. *et al.* (2008) The FHA domain proteins DAWDLE in *Arabidopsis* and SNIP1 in humans act in small RNA biogenesis. *Proc. Natl Acad. Sci. USA*, **105**, 10073–10078.
25. Ren,G.D., Xie,M., Dou,Y.C., Zhang,S.X., Zhang,C. and Yu,B. (2012) Regulation of miRNA abundance by RNA binding protein TOUGH in *Arabidopsis*. *Proc. Natl Acad. Sci. USA*, **109**, 12817–12821.
26. Cai,X.Z., Hagedorn,C.H. and Cullen,B.R. (2004) Human microRNAs are processed from capped, polyadenylated transcripts that can also function as mRNAs. *RNA*, **10**, 1957–1966.
27. Lee,Y., Kim,M., Han,J.J., Yeom,K.H., Lee,S., Baek,S.H. and Kim,V.N. (2004) MicroRNA genes are transcribed by RNA polymerase II. *EMBO J.*, **23**, 4051–4060.
28. Chang,Y.F., Imam,J.S. and Wilkinson,M.E. (2007) The nonsense-mediated decay RNA surveillance pathway. *Anuu. Rev. Biochem.*, **76**, 51–74.
29. Fang,Y.D. and Spector,D.L. (2007) Identification of nuclear dicing bodies containing proteins for microRNA biogenesis in living *Arabidopsis* plants. *Curr. Biol.*, **17**, 818–823.
30. Fujioka,Y., Utsumi,M., Ohba,Y. and Watanabe,Y. (2007) Location of a possible miRNA processing site in SmD3/SmB nuclear bodies in *Arabidopsis*. *Plant Cell Physiol.*, **48**, 1243–1253.
31. Laubinger,S., Sachsenberg,T., Zeller,G., Busch,W., Lohmann,J.U., Rascht,G. and Weigel,D. (2008) Dual roles of the nuclear cap-binding complex and SERRATE in pre-mRNA splicing and microRNA processing in *Arabidopsis* thaliana. *Proc. Natl Acad. Sci. USA*, **105**, 8795–8800.
32. Izaurralde,E., Lewis,J., McGuigan,C., Jankowska,M., Darzynkiewicz,E. and Mattaj,I.W. (1994) A nuclear cap-binding protein complex involved in pre-mRNA splicing. *Cell*, **78**, 657–668.
33. Kim,S., Yang,J.Y., Xu,J., Jang,I.C., Prigge,M.J. and Chua,N.H. (2008) Two cap-binding proteins CBP20 and CBP80 are involved in processing primary microRNAs. *Plant Cell Physiol.*, **49**, 1634–1644.
34. Lee,B.-h., Kapoor,A., Zhu,J. and Zhu,J.-K. (2006) STABILIZED1, a stress-upregulated nuclear protein, is required for pre-mRNA splicing, mRNA turnover, and stress tolerance in *Arabidopsis*. *Plant Cell*, **18**, 1736–1749.

35. Prigge,M.J. and Wagner,D.R. (2001) The *Arabidopsis* SERRATE gene encodes a zinc-finger protein required for normal shoot development. *Plant Cell*, **13**, 1263–1279.
36. Livak,K.J. and Schmittgen,T.D. (2001) Analysis of relative gene expression data using real-time quantitative PCR and the 2(T) (-delta delta C) method. *Methods*, **25**, 402–408.
37. Griffiths-Jones,S., Saini,H.K., van Dongen,S. and Enright,A.J. (2008) miRBase: tools for microRNA genomics. *Nucleic Acids Res.*, **36**, D154–D158.
38. Li,R.Q., Yu,C., Li,Y.R., Lam,T.W., Yiu,S.M., Kristiansen,K. and Wang,J. (2009) SOAP2: an improved ultrafast tool for short read alignment. *Bioinformatics*, **25**, 1966–1967.
39. Bengtsson,H., Irizarry,R., Carvalho,B. and Speed,T.P. (2008) Estimation and assessment of raw copy numbers at the single locus level. *Bioinformatics*, **24**, 759–767.
40. Tusher,V.G., Tibshirani,R. and Chu,G. (2001) Significance analysis of microarrays applied to the ionizing radiation response. *Proc. Natl Acad. Sci. USA*, **98**, 10515–10515.
41. Benjamini,Y. and Hochberg,Y. (1995) Controlling the false discovery rate - a practical and powerful approach to multiple testing. *J. R. Stat. Soc. Ser. B.*, **57**, 289–300.
42. Bezerra,I.C., Michaels,S.D., Schomburg,F.M. and Amasino,R.M. (2004) Lesions in the mRNA cap-binding gene ABA HYPERSENSITIVE 1 suppress FRIGIDA-mediated delayed flowering in *Arabidopsis*. *Plant J.*, **40**, 112–119.
43. Todesco,M., Balasubramanian,S., Cao,J., Ott,F., Sureshkumar,S., Schneeberger,K., Meyer,R.C., Altmann,T. and Weigel,D. (2012) Natural vVariation in biogenesis efficiency of individual *Arabidopsis* thaliana microRNAs. *Curr. Biol.*, **22**, 166–170.
44. Doench,J.G. and Sharp,P.A. (2004) Specificity of microRNA target selection in translational repression. *Genes Dev.*, **18**, 504–511.
45. Elbashir,S.M., Harborth,J., Lendeckel,W., Yalcin,A., Weber,K. and Tuschl,T. (2001) Duplexes of 21-nucleotide RNAs mediate RNA interference in cultured mammalian cells. *Nature*, **411**, 494–498.
46. Martinez,J. and Tuschl,T. (2004) RISC is a 5′ phosphomonoester-producing RNA endonuclease. *Genes Dev.*, **18**, 975–980.
47. Cardon,G.H., Hohmann,S., Nettesheim,K., Saedler,H. and Huijser,P. (1997) Functional analysis of the *Arabidopsis* thaliana SBP-box gene SPL3: a novel gene involved in the floral transition. *Plant J.*, **12**, 367–377.
48. Unte,U.S., Sorensen,A.M., Pesaresi,P., Gandikota,M., Leister,D., Saedler,H. and Huijser,P. (2003) SPL8, an SBP-box gene that affects pollen sac development in *Arabidopsis*. *Plant Cell*, **15**, 1009–1019.
49. Stone,J.M., Liang,X., Nekl,E.R. and Stiers,J.J. (2005) *Arabidopsis* AtSPL14, a plant-specific SBP-domain transcription factor, participates in plant development and sensitivity to fumonisin B1. *Plant J.*, **41**, 744–754.
50. Lee,B.-h., Yu,S.I. and Jackson,D. (2009) Control of plant architecture: the role of Phyllotaxy and Plastochron. *J. Plant Biol.*, **52**, 277–282.
51. Wang,J.W., Czech,B. and Weigel,D. (2009) miR156-Regulated SPL Transcription factors define an endogenous flowering pathway in *Arabidopsis* thaliana. *Cell*, **138**, 738–749.
52. Alonso-Peral,M.M., Li,J.Y., Li,Y.J., Allen,R.S., Schnippenkoetter,W., Ohms,S., White,R.G. and Millar,A.A. (2010) The microRNA159-regulated GAMYB-like genes inhibit growth and promote programmed cell death in *Arabidopsis*. *Plant Physiol.*, **154**, 757–771.
53. Mallory,A.C., Bartel,D.P. and Bartel,B. (2005) MicroRNA-directed regulation of *Arabidopsis* AUXIN RESPONSE FACTOR17 is essential for proper development and modulates expression of early auxin response genes. *Plant Cell*, **17**, 1360–1375.
54. Laufs,P., Peaucelle,A., Morin,H. and Traas,J. (2004) MicroRNA regulation of the CUC genes is required for boundary size control in *Arabidopsis* meristems. *Development*, **131**, 4311–4322.
55. Williams,L., Grigg,S.P., Xie,M.T., Christensen,S. and Fletcher,J.C. (2005) Regulation of *Arabidopsis* shoot apical meristem and lateral organ formation by microRNA miR166g and its AtHD-ZIP target genes. *Development*, **132**, 3657–3668.
56. Aukerman,M.J. and Sakai,H. (2003) Regulation of flowering time and floral organ identity by a microRNA and its APETALA2-like target genes. *Plant Cell*, **15**, 2730–2741.
57. Szarzynska,B., Sobkowiak,L., Pant,B.D., Balazadeh,S., Scheible,W.R., Mueller-Roeber,B., Jarmolowski,A. and Szweykowska-Kulinska,Z. (2009) Gene structures and processing of *Arabidopsis* thaliana HYL1-dependent pri-miRNAs. *Nucleic Acids Res.*, **37**, 3083–3093.
58. Xie,Z.X., Allen,E., Fahlgren,N., Calamar,A., Givan,S.A. and Carrington,J.C. (2005) Expression of *Arabidopsis* MIRNA genes. *Plant Physiol.*, **138**, 2145–2154.
59. Jones-Rhoades,M.W., Bartel,D.P. and Bartel,B. (2006) MicroRNAs and their regulatory roles in plants. *Annu. Rev. Plant Biol.*, **57**, 19–53.
60. Gregory,B.D., O'Malley,R.C., Lister,R., Urich,M.A., Tonti-Filippini,J., Chen,H., Millar,A.H. and Ecker,J.R. (2008) A link between RNA metabolism and silencing affecting *Arabidopsis* development. *Dev. Cell*, **14**, 854–866.
61. Montgomery,T.A. and Carrington,J.C. (2008) Splicing and dicing with a SERRATEd edge. *Proc. Natl Acad. Sci. USA*, **105**, 8489–8490.
62. Sunkar,R., Girke,T., Jain,P.K. and Zhu,J.K. (2005) Cloning and characterization of microRNAs from rice. *Plant Cell*, **17**, 1397–1411.
63. Chen,X.M. (2008) A silencing safeguard: links between RNA silencing and mRNA processing in *Arabidopsis*. *Dev. Cell*, **14**, 811–812.
64. Xie,Z.X., Kasschau,K.D. and Carrington,J.C. (2003) Negative feedback regulation of Dicer-Like1 in *Arabidopsis* by microRNA-guided mRNA degradation. *Curr. Biol.*, **13**, 784–789.